High-Pressure Synthesis of $Sc_5P_{12}N_{23}O_3$ and $Ti_5P_{12}N_{24}O_2$ by Activation of the Binary Nitrides ScN and TiN with NH_4F

Lucien Eisenburger,[a] Valentin Weippert,[a] Oliver Oeckler,*[b] and Wolfgang Schnick*[a]

Abstract: Multinary transition metal nitrides and oxonitrides are a versatile and intriguing class of compounds. However, they have been investigated far less than pure oxides. The compounds $Sc_5P_{12}N_{23}O_3$ and $Ti_5P_{12}N_{24}O_2$ have now been synthesized from the binary nitrides ScN and TiN, respectively, by following a high-pressure high-temperature approach at 8 GPa and 1400 °C. NH_4F acts as a mineralizing agent that supports product formation and crystallization. The starting materials ScN and TiN are seemingly an uncommon choice because of their chemical inertness but, nevertheless, react under these conditions. $Sc_5P_{12}N_{23}O_3$ and $Ti_5P_{12}N_{24}O_2$ crystallize isotypically with $Ti_5B_{12}O_{26}$, consisting of solely vertex-sharing $P(O/N)_4$ tetrahedra forming two independent interpenetrating diamond-like nets that host $TM(O/N)_6$ (TM = Sc, Ti) octahedra. $Ti_5P_{12}N_{24}O_2$ is a mixed-valence compound and shows ordering of Ti^{3+} and Ti^{4+} ions.

A plethora of nitridophosphates was discovered in the last decades. However, only few examples containing transition metals have been described so far which is rather intriguing bearing the ongoing research on transition metal phosphates and their applications in mind.[1–5] Oxonitridophosphates like $M^{I}M^{III}P_3O_9N$ (M^{I} = Na, K, M^{III} = Al, Ga, Cr, Fe, Mn) were the first compounds paving the way for transition metal (oxo)-nitridophosphates.[6,7] By using high-pressure conditions accessible by Walker-type multianvil presses, compounds like MnP_2N_4, CdP_2N_4 and Zn_2PN_3 were synthesized. The metal-containing starting materials were either the *TM* azides (Cd), metal powders (Cd, Mn), or binary nitride (Zn).[8–11] Despite these achievements, no systematic access to this class of compounds was reported as illustrated by the different starting materials. Common chemicals such as azides and nitrides are either too sensitive and detonate on impact or are too inert, respectively. The first systematic approach to a variety of *TM* compounds is represented by metathesis reactions under high-pressure high-temperature conditions as shown for MP_8N_{14} (M = Fe, Co, Ni), $M_{1-x}PO_{3+4x}N_{1-4x}$ ($x \approx 0.05$), $M_{0.75}PO_4$ (M = Zr, Hf) and $Hf_{9-x}P_{24}N_{52-4x}O_{4x}$ ($x \approx 1.84$).[12–15]

High-pressure metathesis with the formation of lithium halides from $LiPN_2$ and *TM* halides, however, features inherent drawbacks. Like many HP/HT syntheses, this approach typically yields microcrystalline powders which impede precise structure elucidation by conventional single-crystal X-ray diffraction. The addition of Li can also pose a problem if the latter is incorporated unintentionally, especially in presence of heavy metal atoms. This combination is rather problematic in terms of structure determination by X-ray methods as it is hard to distinguish between heavy metal vacancies or occupational disorder of the heavy metal and Li.

To facilitate crystal growth of nitridophosphates in high-pressure high-temperature reactions, the addition of small amounts of NH_4Cl to the mixture of starting materials as mineralizer proved to be successful. NH_4Cl most likely aids in reaction and crystal growth by reversible P–N bond cleavage and formation.[16] As shown for group 1, 2 and 13 elements, this kind of activation seems sufficient to provide access to a number of different structures and compounds.[17–19] As previously shown for $AESiP_3N_7$ (AE = Sr, Ba), the capability of NH_4Cl is limited as some starting materials such as Si_3N_4 are less reactive and the decomposition, as well as activation temperatures of the starting materials, may differ significantly; for example, thermal decomposition of P_3N_5 may compete with the activation of Si_3N_4.[20] The question arose if previous findings on the stability of transition metal nitrides remain valid if the mineralizing agent is changed. The starting materials ScN and TiN were chosen because of their refractory character and notorious inertness. For example, TiN is used as a wear- and heat-resistant coating for drill heads.[21] Etching of TiN films is heavily investigated in semiconductor fabrication. Solutions for etching consisting of a source of hydrogen fluoride and an oxidizing agent have proven to be successful in reducing TiN film thickness. The oxidizing agent in these cases is needed to oxidize Ti^{3+} to Ti^{4+} which forms volatile TiF_4, in contrast to non-volatile TiF_3.[22] As the volatility of the fluoride is not an issue in HP/HT syntheses, and we assumed a similar behavior for ScN, we explored the capability of NH_4F as a safe and convenient HF

[a] L. Eisenburger, V. Weippert, Prof. Dr. W. Schnick
Department of Chemistry, University of Munich (LMU)
Butenandtstraße 5–13, 81377 Munich (Germany)
E-mail: wolfgang.schnick@uni-muenchen.de

[b] Prof. Dr. O. Oeckler
Institute for Mineralogy, Crystallography and Materials Science
Leipzig University
Scharnhorststraße 20, 04275 Leipzig (Germany)
E-mail: oliver.oeckler@gmx.de

Supporting information for this article is available on the WWW under https://doi.org/10.1002/chem.202101858

source in reactions yielding the transition-metal oxonitridophosphates $Sc_5P_{12}N_{23}O_3$ and $Ti_5P_{12}N_{24}O_2$.

Both compounds were synthesized at 1400 °C and 8 GPa by using a modified Walker-type multianvil apparatus.[23] Reactions followed the so-called nitride-route using P_3N_5 and *TM*N (*TM* = Sc, Ti) with additional NH_4F as a mineralizing agent [Eqs. (1) and (2)]. PON or TiO_2 were added as oxygen sources. The synthesis of $Ti_5P_{12}N_{24}O_2$, however, was performed with only 0.8 equivalents of TiO_2 as stoichiometric amounts lead to microcrystalline samples and split reflections in the PXRD possibly due to excess oxygen from surface hydrolysis of the BN crucible.

$$5\ ScN + 3\ P_3N_5 + 3\ PON \rightarrow Sc_5P_{12}N_{23}O_3 \quad (1)$$

$$4\ TiN + 4\ P_3N_5 + TiO_2 \rightarrow Ti_5P_{12}N_{24}O_2 \quad (2)$$

Both reactions yielded moisture- and air-resistant crystalline powders with gray and black color for $Sc_5P_{12}N_{23}O_3$ and $Ti_5P_{12}N_{24}O_2$, respectively. More detailed information on the synthesis is given in the Supporting Information.

Structure elucidation was performed by single-crystal X-ray diffraction (SCXRD). Deposition Numbers 2084626 (for $Sc_5P_{12}N_{23}O_3$) and 2084627 (for $Ti_5P_{12}N_{24}O_2$) contain the supplementary crystallographic data for this paper. These data are provided free of charge by the joint Cambridge Crystallographic Data Centre and Fachinformationszentrum Karlsruhe Access Structures service.

Both compounds are isotypic and crystallize in space group $I4_1/acd$ (no. 142) with $Z = 8$ (Table 1). Additional Rietveld refinements indicate that the title compounds are the main constituents of the obtained samples (Figures S2 and S3, Table S9). Both compounds are isotypic to $Ti_5B_{12}O_{26}$.[24] The transition metals are coordinated octahedrally by O/N. The *TM*1$(O/N)_6$ octahedra share one common edge and form pairs in contrast to the *TM*2$(O/N)_6$ octahedra, which are not condensed (Figure 1).

The $P(O/N)_4$ network consists of edge-sharing tetrahedra forming truncated, hollow supertetrahedra which in turn form two separate interpenetrating networks (Figure 2). As differ-

Table 1. Crystallographic data for the single-crystal structure refinements of $Sc_5P_{12}N_{23}O_3$ and $Ti_5P_{12}N_{24}O_2$. Standard deviations are given in parentheses.

formula	$Sc_5P_{12}N_{23}O_3$	$Ti_5P_{12}N_{24}O_2$
molar mass/g mol^{-1}	966.67	979.38
crystal system	tetragonal	
space group	$I4_1/acd$ (no. 142)	
lattice parameters/Å	$a = 12.3598(2)$	$a = 12.1214(2)$
	$c = 24.0151(4)$	$c = 23.8458(5)$
cell volume/Å^3	3668.66(13)	3503.62(14)
formula units/unit cell	8	
density/g cm^3	3.500	3.713
μ/mm^{-1}	2.893	3.369
T/K	296(2)	298(2)
absorption correction	semiempirical	
radiation	$Mo_{K\alpha}$ ($\lambda = 0.71073$ Å)	
F(000)	3760	3792
θ range/°	3.3–36.3	2.9–33.1
total no. of reflections	66300	52537
Indep. reflections [$I \geq 2\sigma(I)$/all]	1971/2226	1567/1676
R_σ, R_{int}	0.0158, 0.0616	0.0108, 0.0353
refined parameters	100	99
Goodness of fit	1.187	1.432
R values [$I \geq 2\sigma(I)$]	$R_1 = 0.0210$	$R_1 = 0.0222$
	$wR_2 = 0.0474$	$wR_2 = 0.0680$
R values (all data)	$R_1 = 0.0264$	$R_1 = 0.0240$
	$wR_2 = 0.0489$	$wR_2 = 0.0690$
$\Delta\rho_{max}$, $\Delta\rho_{min}$/e Å^{-3}	0.552/−0.715	0.921/−1.636

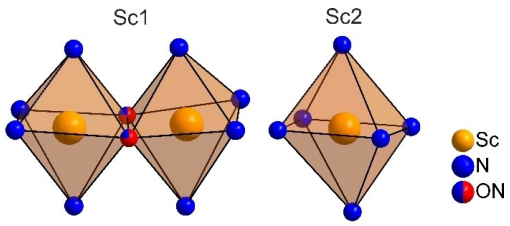

Figure 1. Edge-sharing $ScO_{0.75}N_{5.25}$ and isolated ScN_6 octahedra.

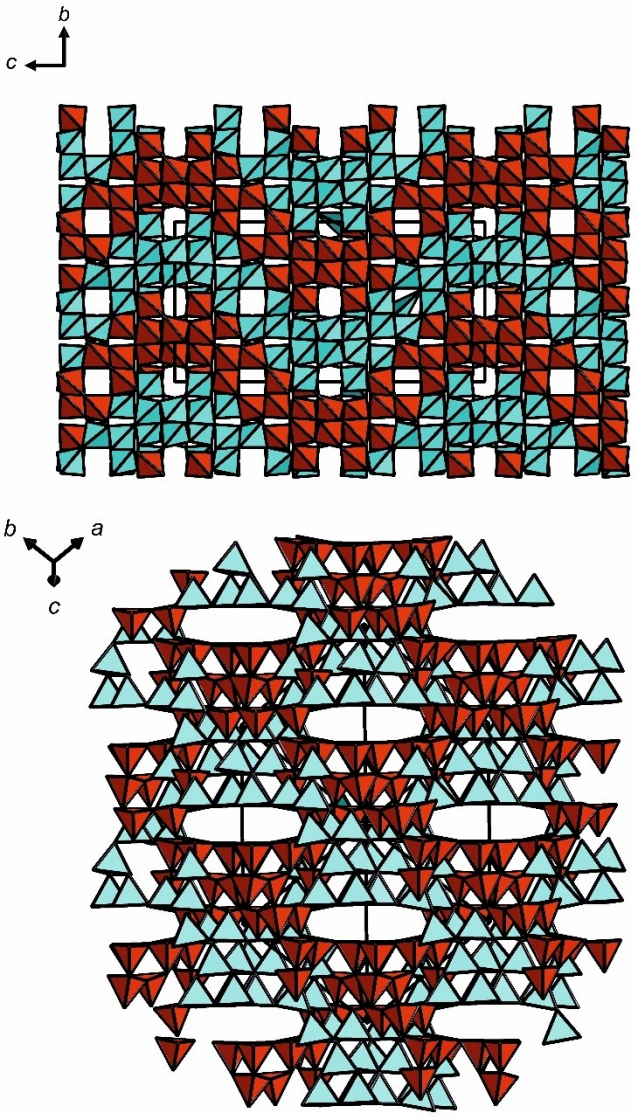

Figure 2. Structure projections viewed from [100] (top) and [111] (bottom). The different diamond-like nets of tetrahedra are colored in red or blue, respectively. *TM* atoms are omitted for clarity.

entiation between O and N is not unambiguous from X-ray data, and ordering of O and N is not possible in terms of charge neutrality, mixed occupied sites were assigned by considering a combination of bond lengths, bond valence sums and charge neutrality. Following this combination, the position O5/N5 and N2 in $Sc_5P_{12}N_{23}O_3$ both showed potential mixed occupation according to BVS but position O5/N5 was considered more likely because of the short P–O/N bond lengths of 1.5722(9) Å and N2 forming unusually large Sc–N distances explained in the following. In $Ti_5P_{12}N_{24}O_2$ assigning mixed occupied positions led to positions O2/N2, O5/N5 and O6/N6 fully consistent with BVS calculations as only these positions showed deviations from the ideal value of 3 for N. Distances *TM*–O/N are between 2.1421(9)–2.4424(9) Å for Sc–O/N and 2.0435(11)–2.2911(11) Å for Ti–O/N (Tables S6 and S7). Both compounds exhibit rather large interatomic distances concerning the *TM*2 position. In the equatorial plane of the *TM*2$(O/N)_6$ octahedron, the distances Sc2–N2 (2.4424(9) Å) deviate quite significantly from those in ScN (2.25 Å).[25] The Ti2 position exhibits distances Ti–$(O_{0.15}N_{0.85})$ of 2.2911(11) Å which are also larger than expected with respect to TiN or rutile-type TiO_2, where they are 2.13 and 1.81–2.06 Å, respectively.[26,27] The long interatomic distances result in a "rattling" effect which is reflected by low BVS values for these positions and their rather large and prolate displacements ellipsoids (Figure S1). The BVS values are 2.42 for Sc2 and 2.64 for Ti2 instead of the expected values of 3 for Sc and 4 for Ti2.

The chemical compositions of $Sc_5P_{12}N_{23}O_3$ and $Ti_5P_{12}N_{24}O_2$ are supported by energy-dispersive X-ray spectroscopy (Table S8) and FTIR spectra indicate the absence of N–H groups (Figure S4). Scanning transmission electron microscope high-angle annular dark-field (STEM-HAADF) images correspond well to structure projections (Figure 3).

In order to confirm the presence of both Ti^{3+} and Ti^{4+} in $Ti_5P_{12}N_{24}O_2$, UV-Vis absorption spectra and magnetic measurements were performed. UV-Vis spectra show a broad absorption band centered at 420 nm, which corresponds well with the presence of Ti^{3+} (Figure S6).[28] Figure 4 shows the magnetic susceptibility with a linear paramagnetic behavior for temperatures >200 K. The fit indicates an effective paramagnetic moment of $\mu_{eff} = 1.7(1)\ \mu_B$ for each Ti cation on Wyckoff position 32 *g* assuming Ti^{4+} on Wyckoff position 8*b*. This is in agreement with the theoretical spin-only value for Ti^{3+} with $\mu_{eff} = 1.73\ \mu_B$.[29] Below 200 K, the curve deviates from Curie–Weiss behavior with a continuously increasing magnetic moment. Magnetization isotherms at 300 K with purely paramagnetic behavior and with a small saturation effect at 2 K towards higher fields are shown in the bottom part of Figure 4.

In analogy to $Ti_5B_{12}O_{26}$, we could assign crystallographic sites for Ti^{3+} and Ti^{4+} according to the presence of both valence states.[24] Although the similarity of the ordering of Ti^{3+} and Ti^{4+} is quite remarkable given the fact that the composition of the tetrahedral network is completely altered.

The optical bandgap of $Ti_5P_{12}N_{24}O_2$ was approximated by converting reflectance spectra to the Kubelka-Munk function and calculating a Tauc plot under the assumption of a direct bandgap. Linear regression between 2.1 and 3.1 eV was used to determine the inflection point yielding a bandgap of about 1.6 eV.[30,31] In the same way, the optical bandgap of $Sc_5P_{12}N_{23}O_3$ was estimated by linear regression between 4.0 and 4.5 eV and determined as a direct bandgap of 3.8 eV (Figure S7).

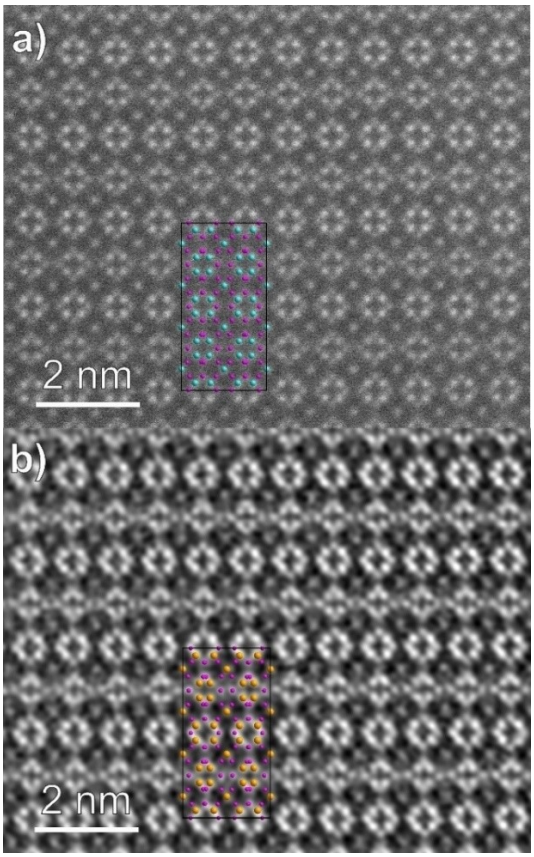

Figure 3. STEM-HAADF images of a) $Ti_5P_{12}N_{24}O_2$ and b) $Sc_5P_{12}N_{23}O_3$ with structure projections as overlays (Ti: blue, Sc: orange, P: violet, O/N omitted for clarity).

Conclusion

The oxonitridophosphates $Ti_5P_{12}N_{24}O_2$ and $Sc_5P_{12}N_{23}O_3$ have been synthesized with NH_4F as a mineralizing agent by high-pressure high-temperature synthesis. The use of NH_4F as a mineralizing agent seems promising to access a variety of yet unknown compounds. The mechanistic reasons for the apparent superiority of NH_4F in contrast to NH_4Cl, still need to be investigated and will certainly be interesting. The presence of Ti^{3+} and Ti^{4+} in $Ti_5P_{12}N_{24}O_2$ was derived from crystal-chemical considerations and confirmed by magnetic measurements as well as UV-Vis spectroscopy.

The easy accessibility of *TM* oxonitridophosphates from binary nitrides constitutes a significant progress in the exploration of multinary nitride network structures. This, in turn, is now offering a new scope of properties for nitridophophates like magnetic properties for spintronic applications as diluted magnetic semiconductors, for example, by substoichiometric doping with *TM*.[33] The incorporation of *TM* in nitridophophates

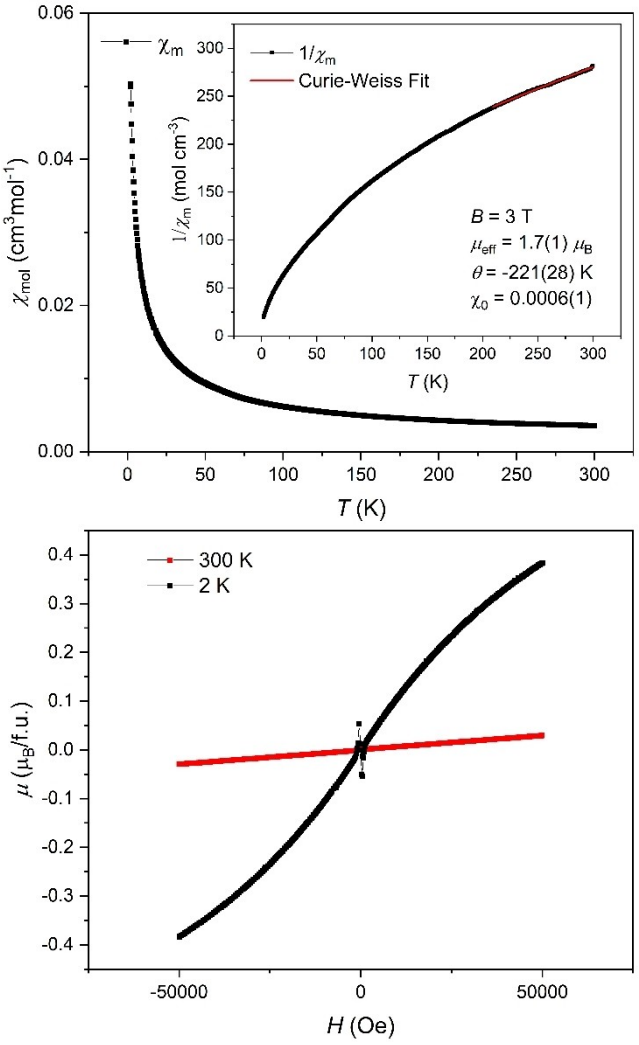

Figure 4. Top: Magnetic susceptibility of $Ti_5P_{12}N_{24}O_2$ and inverse magnetic susceptibility (inset) with an extended Curie-Weiss fit (red) and bottom: Magnetization isotherm of $Ti_5P_{12}N_{24}O_2$ at 300 (red) and 2 K (black). At low field strengths, a small superconducting impurity, most likely of TiN, is revealed ($T_c = 5.6$ K).[32]

also allows the metal cations to be mixed-valent, as shown for $Ti_5P_{12}N_{24}O_2$, which could also be formulated as $Ti^{III}_4Ti^{IV}P_5N_{24}O_2$ for clarification. This leads to significantly smaller bandgaps compared to group 1 or group 2 nitridophosphates, which, so far, result in ultrawide-bandgap semiconductors. Research on $Ti_5P_{12}N_{24}O_2$ regarding solar power harvesting and photocatalysis seems intriguing judging by its bandgap of 1.6 eV and the fact that TiO_2 and TiN are both intensively investigated in those fields.[34–37]

The next obstacle to overcome are syntheses of oxygen-free *TM* nitrides, by employing NH_4F and the binary *TM* nitrides. Thus, delivering straightforward access to a group of multinary nitrides which are, despite their projected potential applications, scarcely investigated.

Acknowledgments

Financial support by the Deutsche Forschungsgemeinschaft (DFG, SCHN 377/18-1, OE 513/6-1) is gratefully acknowledged. We thank Dr. Peter Mayer for single-crystal data collection, Dr. Steffen Schmidt and Lisa Gamperl for SEM investigations and Prof. Dr. Dirk Johrendt for his support and enabling us to perform magnetic measurements. Open Access funding enabled and organized by Projekt DEAL.

Conflict of Interest

The authors declare no conflict of interest.

Keywords: high-pressure chemistry · mixed-valent compounds · nitrides · solid-state synthesis · transition metals

[1] H. S. Ahn, T. D. Tilley, *Adv. Funct. Mater.* **2013**, *23*, 227–233.
[2] B. Lung-Hao Hu, F. Y. Wu, C. Te Lin, A. N. Khlobystov, L. J. Li, *Nat. Commun.* **2013**, *4*, 1–7.
[3] X. Shen, Q. Zhou, M. Han, X. Qi, B. Li, Q. Zhang, J. Zhao, C. Yang, H. Liu, Y.-S. Hu, *Nat. Commun.* **2021**, *12*, 2848.
[4] S. Y. Chung, J. T. Bloking, Y. M. Chiang, *Nat. Mater.* **2002**, *1*, 123–128.
[5] B. Kang, G. Ceder, *Nature* **2009**, *458*, 190–193.
[6] S. D. Kloß, W. Schnick, *Angew. Chem. Int. Ed.* **2019**, *58*, 7933-7944; *Angew. Chem.* **2019**, *131*, 9158–9161.
[7] W. Feldmann, *Z. Chem.* **1987**, *27*, 182–183.
[8] S. J. Sedlmaier, M. Eberspächer, W. Schnick, *Z. Anorg. Allg. Chem.* **2011**, *637*, 362–367.
[9] F. Karau, O. Oeckler, F. Schäfers, R. Niewa, W. Schnick, *Z. Anorg. Allg. Chem.* **2007**, *633*, 1333–1338.
[10] F. J. Pucher, F. Hummel, W. Schnick, *Eur. J. Inorg. Chem.* **2015**, *2015*, 1886–1891.
[11] F. J. Pucher, F. W. Karau, J. Schmedt auf der Günne, W. Schnick, *Eur. J. Inorg. Chem.* **2016**, *2016*, 1497–1502.
[12] S. D. Kloß, A. Weis, S. Wandelt, W. Schnick, *Inorg. Chem.* **2018**, *57*, 4164–4170.
[13] S. D. Kloß, S. Wandelt, A. Weis, W. Schnick, *Angew. Chem. Int. Ed.* **2018**, *57*, 3192–3195; *Angew. Chem.* **2018**, *130*, 3246–3249.
[14] S. D. Kloß, O. Janka, T. Block, R. Pöttgen, R. Glaum, W. Schnick, *Angew. Chem. Int. Ed.* **2019**, *58*, 4685-4689; *Angew. Chem.* **2019**, *131*, 4733–4737.
[15] S. D. Kloß, N. Weidmann, W. Schnick, *Eur. J. Inorg. Chem.* **2017**, *2017*, 1930–1937.
[16] D. Baumann, W. Schnick, *Inorg. Chem.* **2014**, *53*, 7977–7982.
[17] S. Wendl, L. Eisenburger, P. Strobel, D. Günther, J. P. Wright, P. J. Schmidt, O. Oeckler, W. Schnick, *Chem. Eur. J.* **2020**, *26*, 7292–7298.
[18] A. Marchuk, V. R. Celinski, J. Schmed auf der Günne, W. Schnick, *Chem. Eur. J.* **2015**, *21*, 5836–5842.
[19] L. Neudert, F. Heinke, T. Bräuniger, F. J. Pucher, G. B. Vaughan, O. Oeckler, W. Schnick, *Chem. Commun.* **2017**, *53*, 2709–2712.
[20] L. Eisenburger, O. Oeckler, W. Schnick, *Chem. Eur. J.* **2021**, *27*, 4461–4465.
[21] E. Santecchia, A. M. S. Hamouda, F. Musharavati, E. Zalnezhad, M. Cabibbo, S. Spigarelli, *Ceram. Int.* **2015**, *41*, 10349–10379.
[22] Y. Lee, S. M. George, *Chem. Mater.* **2017**, *29*, 8202–8210.
[23] H. Huppertz, *Z. Kristallogr.* **2004**, *219*, 330–338.
[24] A. Haberer, H. Huppertz, *J. Solid State Chem.* **2009**, *182*, 484–490.
[25] B. Hájek, V. Brožek, P. H. Duvigneaud, *J. Less-Common Met.* **1973**, *33*, 385–386.
[26] M. N. Khan, K. Shahzad, J. Bashir, *J. Phys. D: Appl. Phys.* **2008**, *41*, 085409.
[27] S. Inamura, K. Nobugai, F. Kanamaru, *J. Solid State Chem.* **1987**, *68*, 124–127.
[28] X. Meng, B. Huang, X. Ma, Z. Wang, Z. Zheng, J. Wang, X. Qin, X. Zhang, Y. Dai, *CrystEngComm* **2014**, *16*, 6538–6541.
[29] H. Lueken, *Magnetochemie*, Vieweg + Teubner, Wiesbaden, **1999**.
[30] J. Tauc, R. Grigorovici, A. Vancu, *Phys. Status Solidi* **1966**, *15*, 627–637.
[31] E. A. Davis, N. F. Mott, *Philos. Mag.* **1970**, *22*, 903–922.

[32] W. Spengler, R. Kaiser, A. N. Christensen, G. Müller-Vogt, *Phys. Rev. B* **1978**, *17*, 1095–1101.
[33] M. H. Kane, S. Gupta, I. T. Ferguson, in *Rare Earth and Transition Metal Doping of Semiconductor Materials: Synthesis, Magnetic Properties and Room Temperature Spintronics*, Elsevier, **2016**, pp. 315–370.
[34] Y. Bai, I. Mora-Seró, F. De Angelis, J. Bisquert, P. Wang, *Chem. Rev.* **2014**, *114*, 10095–10130.
[35] H. Chen, C. E. Nanayakkara, V. H. Grassian, *Chem. Rev.* **2012**, *112*, 5919–5948.
[36] B. Yoo, K. J. Kim, Y. H. Kim, K. Kim, M. J. Ko, W. M. Kim, N. G. Park, *J. Mater. Chem.* **2011**, *21*, 3077–3084.
[37] S. Ishii, S. L. Shinde, W. Jevasuwan, N. Fukata, T. Nagao, *ACS Photonics* **2016**, *3*, 1552–1557.

Manuscript received: May 26, 2021
Accepted manuscript online: August 18, 2021
Version of record online: August 31, 2021

